Risks from climate extremes change differently from 1.5°C to 2.0°C depending on rarity

Viatcheslav V. Kharin, Greg Flato, Xuebin Zhang, Nathan P. Gillett, Francis W. Zwiers & Kevin Anderson

2018

Pacific Climate Impacts Consortium (PCIC)

PCIC Publications

Original citation:

Kharin, V. V., Flato, G., Zhang, X., Gillett, N. P., Zwiers, F. W., & Anderson, K. (2018). Risks from climate extremes change differently from 1.5°C to 2.0°C depending on rarity. *Earth's Future, 6*(5), 704–715.
https://doi.org/10.1002/2018EF000813

AGU100 ADVANCING EARTH AND SPACE SCIENCE

Earth's Future

RESEARCH ARTICLE
10.1002/2018EF000813

Special Section:
Avoiding Disasters: Strengthening Societal Resilience to Natural Hazards

Risks from Climate Extremes Change Differently from 1.5°C to 2.0°C Depending on Rarity

V. V. Kharin[1], G. M. Flato[1], X. Zhang[2], N. P. Gillett[1], F. Zwiers[3], and K. J. Anderson[2]

[1]Canadian Centre for Climate Modelling and Analysis, Climate Research Division, Environment and Climate Change Canada, University of Victoria, Victoria, British Columbia, Canada, [2]Climate Data and Analysis Section, Climate Research Division, Environment and Climate Change Canada, Toronto, Ontario, Canada, [3]Pacific Climate Impacts Consortium, University of Victoria, Victoria, British Columbia, Canada

Abstract Parties to the United Nations Framework Convention on Climate Change have agreed to hold the "increase in global average temperature to well below 2°C above preindustrial levels and to pursue efforts to limit the temperature increase to 1.5°C." Comparison of the costs and benefits for different warming limits requires an understanding of how risks vary between warming limits. As changes in risk are often associated with changes in exposure due to projected changes in local or regional climate extremes, we analyze differences in the risks of extreme daily temperatures and extreme daily precipitation amounts under different warming limits. We show that global warming of 2°C would result in substantially larger changes in the probabilities of the extreme events than global warming of 1.5°C. For example, over the global land area, the probability of a warm extreme that occurs once every 20 years on average in the current climate is projected to increase 130% and 340% at the 1.5°C and 2.0°C warming levels, respectively (median values). Moreover, the relative changes in probability are larger for rarer, more extreme events, implying that risk assessments need to carefully consider the extreme event thresholds at which vulnerabilities occur.

Key Points:
- Changes in the probabilities of extreme events are substantially larger under 2°C global warming than under 1.5°C global warming
- Relative changes in probability in a warmer world are larger for rarer, more extreme events

Supporting Information:
- Supporting Information S1

Correspondence to:
X. Zhang,
xuebin.zhang@canada.ca

Citation:
Kharin, V. V., Flato, G. M., Zhang, X., Gillett, N. P., Zwiers, F., & Anderson, K. J. (2018). Risks from climate extremes change differently from 1.5°C to 2.0°C depending on rarity. *Earth's Future*, *6*, 704–715. https://doi.org/10.1002/2018EF000813

Received 5 JAN 2018
Accepted 16 APR 2018
Accepted article online 20 APR 2018
Published online 17 MAY 2018

1. Introduction

Limiting global temperature increase to levels that would prevent "dangerous anthropogenic interference with the climate system" is the ultimate aim of the United Nations Framework Convention on Climate Change and its 195-country membership (United Nations Framework Convention on Climate Change, 2015). The Paris Agreement sets a limit on global mean temperature change of 2°C and an aspirational limit of 1.5°C relative to preindustrial levels. Although the challenge of rapidly reducing global greenhouse gas emissions so as to not exceed these limits is daunting (e.g., Rogelj et al., 2015), the impacts on human and natural systems can be profound even at such modest warming levels. The greatest direct impacts on human society and natural systems from climate variability and change frequently result from climate and weather extremes (Easterling et al., 2000; IPCC, 2012). For example, public health and infrastructure design are two aspects of human society that are affected. Heat waves often have direct public health consequences, and changes in their intensity and duration have become an important concern for public health officials (Dunne et al., 2013; Li et al., 2017; Pal & Eltahir, 2015). Changes in heavy rainfall have important consequences for multiple aspects of infrastructure design (drainage systems, roof and building envelop systems, large water control structures, etc.), with the result that engineers are increasingly trying to understand and project changes in infrastructure design values. Forests are a class of natural systems that are affected. For example, increases in winter minimum temperatures pose significant threats to North American forests from southern pine beetle (Lesk et al., 2017).

Annual daily maximum (TXx) and daily minimum (TNn) temperatures and annual maximum 1-day precipitation (RX1day) are among the simplest indicators of climate extremes. Their past changes and the causes of those changes, as well as their future projections, have been widely studied (Donat et al., 2013; Handmer et al., 2012; Kharin et al., 2013; Kim et al., 2016; Min et al., 2011; Zhang et al., 2013; Zwiers et al., 2011). The observed and modeled changes in these annual extremes are in general agreement at the global scale, despite some limitations in observations and modeled extremes. This consistency provides a measure of confidence in future projections, at least on a large scale. The modeled trends in annual maximum and minimum daily temperatures in the second half of the 20th century are consistent with both reanalyses and station-based estimates (Sillmann et al., 2013), although modeled warming in the warm extremes is somewhat slower than observed and that in the cold extremes is somewhat faster than observed. Annual maximum

1-day precipitation amount has increased with surface temperature warming at a rate of about 7% per 1°C global mean temperature, close to that at which the water-holding capacity of the troposphere increases following the Clausius-Clapeyron relationship (Westra et al., 2013). This rate of change is reproduced in multimodel simulated projections of changes in the extreme precipitation (Kharin et al., 2013). The simulated effects of anthropogenic forcing on extreme precipitation are also consistent with observed changes on average over Northern Hemisphere land (Zhang et al., 2013).

Most studies examine changes in projected climate at a specific time in the future conditional on one or more greenhouse gas and aerosol forcing scenarios. In contrast, the focus of the Paris agreement is on global mean warming limits. It therefore becomes more important to quantify projected changes in terms of temperature limits rather than emission scenarios. To the extent that regional changes in extreme temperature and precipitation scale with global temperature across emission scenarios, it is possible to link regional or national impacts to specified global warming limits (Seneviratne et al., 2016).

Ultimately, risk, which represents the combined effect of the likelihood of an event and its consequences, results from a complex confluence of factors including exposure (such as changes in population and wealth) and vulnerability (Handmer et al., 2012; Leonard et al., 2014; Oppenheimer et al., 2014). Nevertheless, a simple framework that compares only the probabilities of temperature and precipitation extremes associated with a 2°C warming limit versus a 1.5°C limit may be useful. This is because its conceptual simplicity aids understanding by making assumptions explicit and because a clear theoretical foundation provides an important point of comparison for more complex approaches. Here we use the ratio of the probabilities of occurrence of a predefined extreme event at different levels of global warming to illustrate the differential impacts of different levels of warming on the rarity of extreme events defined with simple indicators of climate extremes. These probability ratios are referred to as "risk ratios" in the event attribution literature (e.g., NAS 2016), even though they do not characterize relative risks in a very comprehensive way. Nevertheless, this ratio can be interpreted as a lower bound to relative changes in the expected losses due to the extremes provided that the consequences of extreme events of a fixed intensity do not decrease with warming, consistent with expectations. This simple concept may therefore provide a powerful tool for high-level cost-benefit analysis.

2. Data and Methods

2.1. Data

We use annual maximum values of daily precipitation amount (RX1day), daily maximum temperature (TXx), and daily minimum temperature (TNn) simulated by climate models participating in the Coupled Model Intercomparison Project Phase 5 (CMIP5, Taylor et al., 2012). The simulations include both the historical simulations (years 1860–2005) and future climate projections (years 2006–2100) under different greenhouse gas and aerosol forcing scenarios, namely, RCP 2.6, 4.5, and 8.5 (see ref. van Vuuren et al., 2011 for details). The preindustrial climate is represented by model simulations of the period 1861–1880. A list of the models used is provided in Table S1 in the supporting information.

2.2. Methodology

We follow the approach of Kharin et al. (2013) and references therein for the analysis of climate extremes. Generalized extreme value (GEV) distributions (Coles, 2001) are fitted to annual temperature and precipitation extremes at every grid point using data from the historical (years 1860–2005) and three RCP simulations, RCP2.6, RCP4.5, and RCP8.5 (years 2005–2100) combined.

The (cumulative) GEV distribution function is given by

$$F(x;\mu,\sigma,\xi)=\begin{cases}\exp\left[-\exp\left(-\dfrac{x-\mu}{\sigma}\right)\right], \xi=0,\\ \exp\left[-\left(1+\xi\dfrac{x-\mu}{\sigma}\right)^{-\frac{1}{\xi}}\right], \xi\neq 0, 1+\xi\dfrac{x-\mu}{\sigma}>0,\end{cases} \quad (1)$$

where μ is the location parameter, σ is the (positive) scale parameter, and ξ is the shape parameter. These parameters are estimated by the method of maximum likelihood. Here we assume that the

location parameter and the log of the scale parameter depend linearly on the global mean temperature change ΔT as

$$\begin{aligned} \mu_{\Delta T} &= \mu_0 + \mu_1 \Delta T, \\ \log\sigma_{\Delta T} &= \log\sigma_0 + \sigma_1 \Delta T, \end{aligned} \tag{2}$$

A log linear dependence of the scale parameter on the global mean temperature change ensures that the scale parameter remains positive for any value of ΔT with the dependence of σ on ΔT being approximately linear in the vicinity of $\Delta T = 0$. We considered the possibility that the shape parameter ξ might also vary with global mean temperature but found that allowing it to be linearly dependent on ΔT did not improve the goodness of fit as judged by standard likelihood ratio tests, suggesting little appreciable change in the shape parameters due to warming. More flexible statistical models with additional quadratic terms in the dependence of the location and scale parameters in (2) were also tested but proved to be of little additional benefit for the goodness of fit according to the likelihood ratio tests (Table S2).

The global mean temperature change is defined here relative to the global mean temperature in years 1861–1880 of the historical simulations, which is a period with little volcanic activity and when the cumulative emissions of greenhouse gases from human activity remain small compared to the present. Since we are primarily interested in the dependence of the distribution of annual extremes on prevailing time-averaged temperature conditions, interannual variability in the global mean annual temperature time series in each model is suppressed by applying a 21-year moving average when computing the global mean temperature changes ΔT. The intercept coefficients μ_0 and σ_0 and the constant shape parameter ξ characterize the distribution of annual extremes for $\Delta T = 0$, that is, in years 1861–1880 referred to as the "preindustrial" era. The results are largely insensitive to the choice the base period as nearly identical results were obtained for the 1986–2005 baseline.

The five parameters in (1) and (2), μ_0, μ_1, σ_0, σ_1, and ξ are first estimated for each of 26 models listed in Table S1 at every grid point on each model's native grid. Data for 26 models were available for the RCP4.5 and RCP8.5 scenarios but only for 18 models for the RCP2.6 scenario. A single model simulation for each forcing scenario is used in the present study. Most of the results presented in the main text are obtained for samples obtained by joining together historical simulations (years 1860–2005) and all three RCP simulations, RCP2.6, RCP4.5, and RCP8.5 (years 2006–2100). For the models that submitted simulations for all three RCP scenarios, the combined sample therefore consists of 401 annual extremes for each grid box (146 years for the historical period plus 3×85 years for three RCP simulations). For the models without RCP2.6 simulations the combined sample size is 306. To test the dependence of the results on the RCP scenario, the GEV distribution was also fitted to samples of annual extremes in the historical period and only one of the three RCP scenarios, in which case the sample size is 231.

Having fitted the GEV distribution, changes in return values for a given return period or changes in return periods for a given present-day era return value (and the corresponding changes in probability of extreme events) relative to a fixed temperature level (such as the present or preindustrial) can be estimated by varying ΔT within the range of changes simulated by the CMIP5 models (including ΔT = 0, 0.5, 1.0, 1.5, and 2.0°C). Multimodel ensemble statistics are obtained by interpolating the extreme value statistics estimated for each model on their native grids onto a common regular $1.5° \times 1.5°$ latitude-longitude grid. We use multimodel median values, which are less sensitive to outliers than the multimodel mean values. Regional statistics are also obtained by computing spatial medians rather than spatial means.

The risk ratio is defined as the ratio of the probability of an extreme event for a specified value of ΔT to that for $\Delta T = 1.0$°C global mean temperature increase. We consider 1°C warming as being representative of the current climate since the temperature of the warmest year on record, 2016, is about 1.1°C above preindustrial levels (WMO, 2017). The regional estimates of changes in risk ratio are obtained by computing regional median estimates of the extreme value probabilities at a specified value of ΔT and comparing it to the probability of an extreme event at $\Delta T = 1.0$°C.

The uncertainty of model results is assessed by computing the multimodel interquartile (25%–75%) range that contains estimates for half of the models. For example, the shading in Figure 4b indicates the 25%–75% multimodel range of projected risk ratios over land.

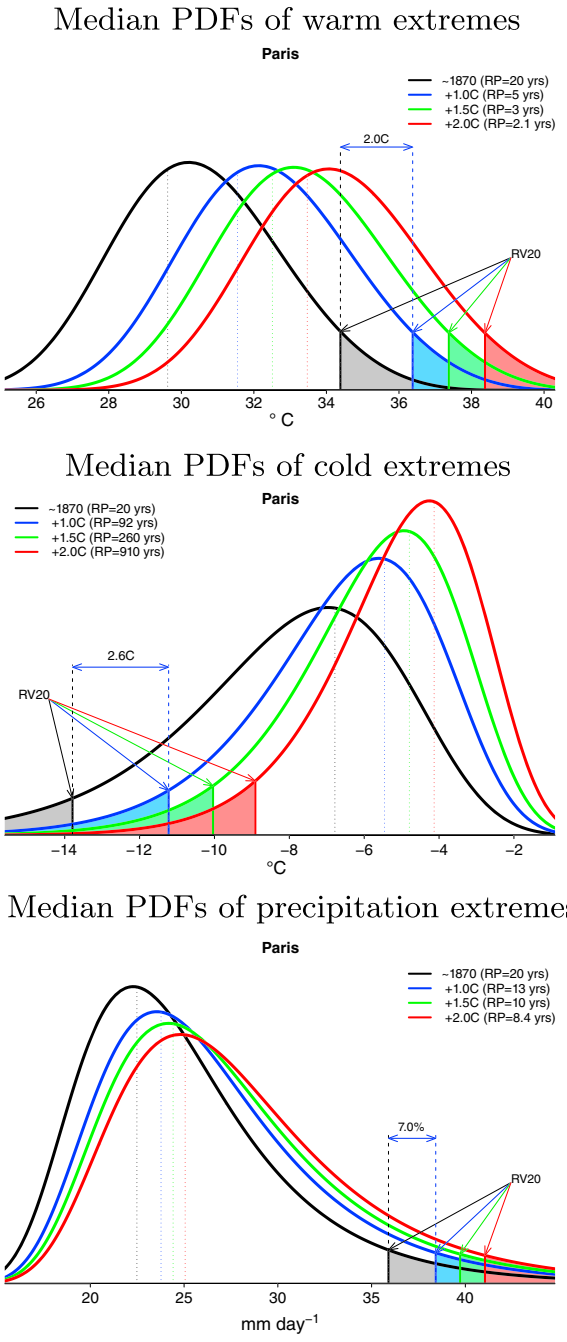

Figure 1. Multimodel median probability density functions (PDFs) for (top) annual warm and (middle) cold temperature extremes and (bottom) annual daily precipitation extremes for the grid box that contains Paris, France, at different global warming levels. PDFs estimated for the preindustrial climate (black curves), and for 1°C (blue), 1.5°C (green), and 2°C (red) global warming are shown. The vertical dotted lines show the value of the location parameter for each distribution function, while the shaded area represents 1 of 20 of the areas under each distribution and so demarcates the 20-year return value. Changes in 20-year return values corresponding to 1°C global warming relative to preindustrial (defined here as 1861–1880) are also indicated for each quantity (1.9°C for warm temperature extremes, 2.0°C for cold temperature extremes, and 5.3% for precipitation extremes). Legends indicate expected return periods at different warming levels of extreme events that occur once every 20 years in the preindustrial climate.

3. Results

3.1. Changes in the Probability Distribution of Extremes

In the case of both temperature and precipitation extremes, there is an overall shift toward higher values, corresponding to an increase in the location parameter, reflecting warming in the case of temperature and an increase in intensity in the case of precipitation. Over land there is generally little change in the scale parameter for warm extremes. The scale parameter decreases for cold extremes in areas where snow and sea ice retreat, suggesting moderately lower variability in the warmer world in these areas but little change elsewhere. On the other hand, the scale parameter for extreme precipitation increases, indicating higher variability. These results are also insensitive to the use of data from different RCP scenarios (see Figures S5–S7 in the supporting information).

As an illustration, Figure 1 shows the multimodel median GEV distribution for the model grid box containing the birthplace of the Paris Agreement for different levels of global mean warming for annual maximum temperature, annual minimum temperature, and annual maximum 24-hr precipitation. These multimodel probability density functions (PDFs) are estimated by first separately fitting GEV distributions to individual model runs and then taking the median values of the estimated GEV distribution parameters from the available model runs as the parameters for the multimodel PDFs. Note that the risk ratios computed from these "median" PDFs could be slightly different from the median values of the risk ratios computed from PDFs fitted to individual model runs. The latter are used when discussing changes in the risks (Figures 2–4 and S4–S7 and Table 1). We see that for Paris, a preindustrial climate (1861–1880) 1-in-20-year warm temperature extreme occurs about 4 times more frequently (about once every 5 years) in the climate that is 1°C warmer than preindustrial. For 2°C global warming, the event occurs once every 2 years on average, that is, 10 times more frequently. Changes in cold extremes are such that the preindustrial 1-in-20-year event becomes a 1-in-50-year event in the current climate and less than a 1-in-200-year event for global warming of 2°C or greater (though we note that the estimates of such large return period values are associated with larger uncertainty). Preindustrial 20-year extreme precipitation events become 14-year events (i.e., 33% increase in probability) in the current climate and 10-year events (100% increase in probability) at 2°C global temperature increase.

3.2. Risk Ratios Under the 1.5°C and 2.0°C Warming Limits

Figure 2 shows maps of the risk ratios for annual warm or cold temperature extremes and precipitation extremes that occur once in 20 years in the current climate (1°C) as compared to those at the 1.5°C and 2°C global temperature warming levels (corresponding to an additional global mean warming of 0.5°C and 1°C above the present level). The risk ratio comparing the likelihood of warm extremes at the 1.5°C warming level relative to the present level is larger than one everywhere, which indicates more frequent occurrence of those extremes, with larger values in lower latitudes and the highest values over oceans. Natural variability over lower latitudes and oceans is relatively low compared to the projected future changes so that shifts in narrow distributions result in

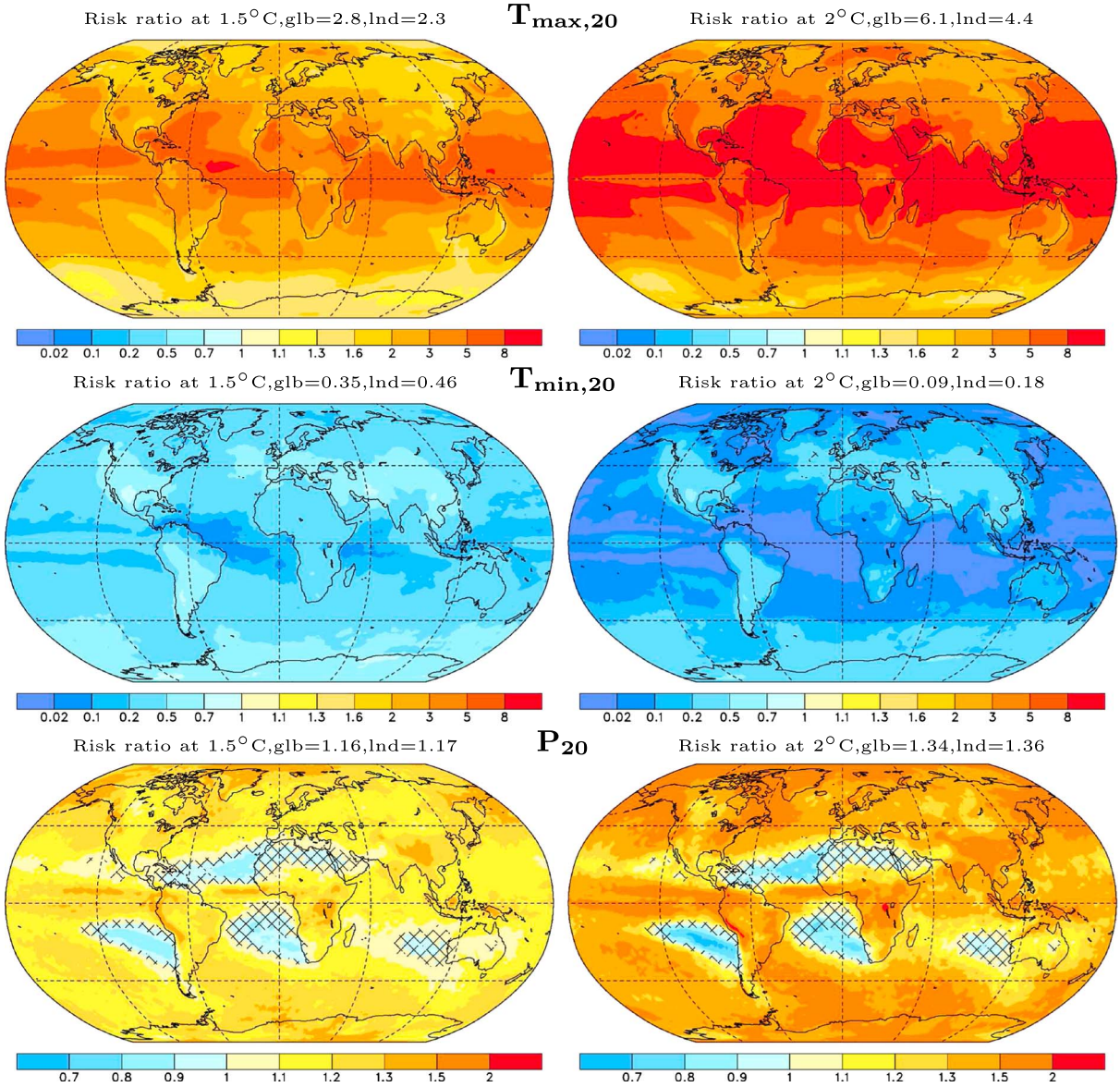

Figure 2. Multimodel median risk ratio for warm and cold temperature extremes and precipitation extremes at (left) 1.5°C and (right) 2°C global warming. The extremes are defined as annual maximum daily maximum and annual minimum daily minimum temperatures as well as annual maximum 1-day precipitation accumulations that are expected to occur once every 20 years in the current climate (1.0°C global warming relative to preindustrial). Global and land median risk ratio values are indicated in the titles.

large changes in probabilities of extreme events and therefore of their higher risk ratios. The land median risk ratio is 2.3, or a 130% increase in the probability of occurrence. The risk ratio for the warm extremes at the 2.0°C warming level follows a similar pattern but has much larger values. The land median risk ratio is 4.4, which translates to a 340% increase in the frequency of occurrence of warm extremes over land relative to their rates of occurrence at 1°C, with 210% of that frequency increase occurring as a consequence of global warming level increasing from 1.5°C to 2.0°C, relative to preindustrial.

As the globe warms, cold extremes become less frequent. The risk ratio for the 20-year cold extremes at the 1.5°C warming level is less than one everywhere, with a stronger decrease toward lower latitudes. The land median risk ratio is 0.45, or a decrease in the risk of the cold extremes by more than half. The risk ratio for the cold extremes is reduced further at the 2.0°C warming level. The land median risk ratio is 0.17, an 83% reduction in frequency from present levels, and a further 28% reduction compared with that at 1.5°C

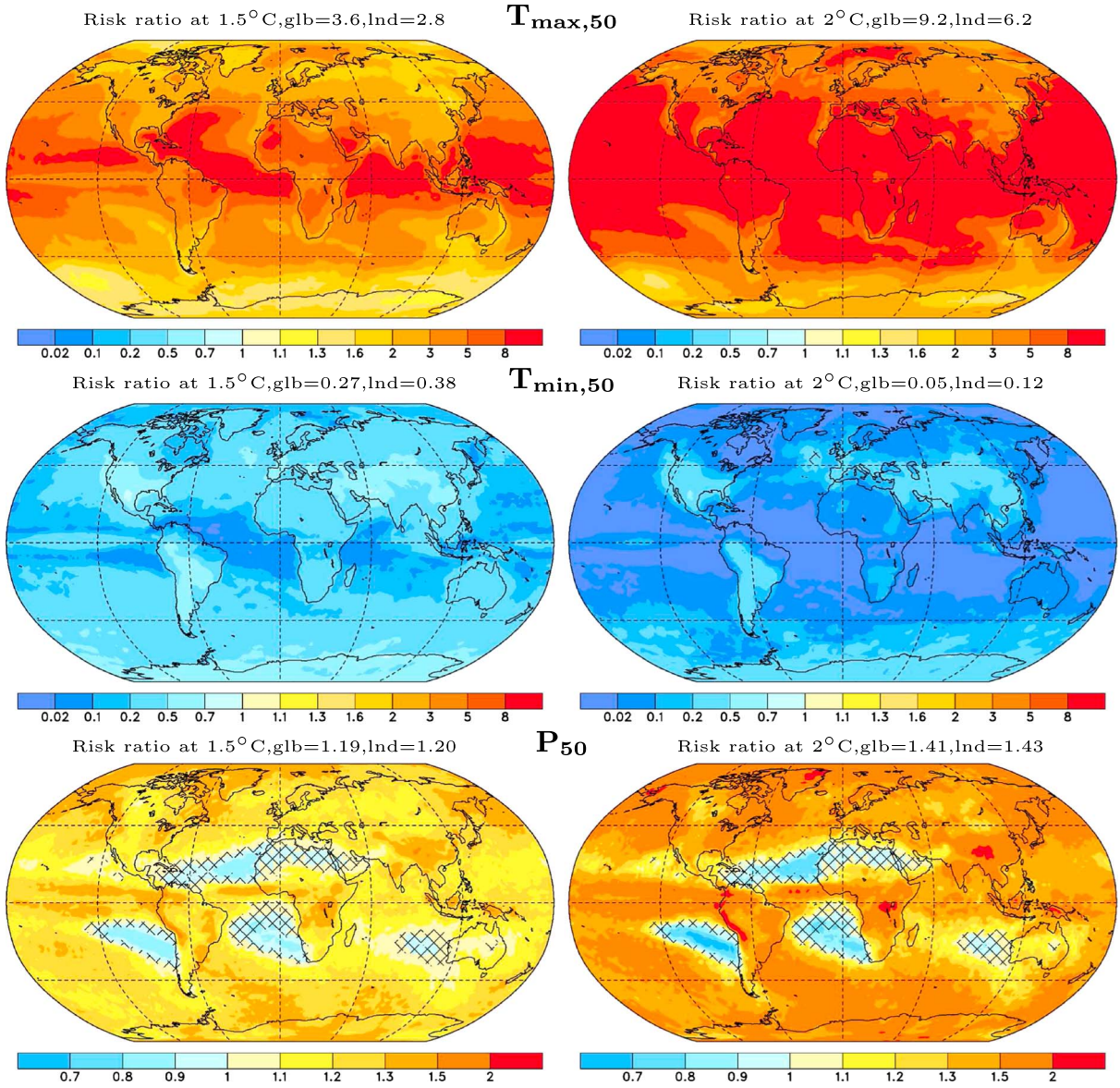

Figure 3. Same as Figure 2 but for 50-year events.

warming. The risk ratio for extreme precipitation is generally larger than one over most land areas when comparing the climate at the 1.5°C global warming level with that at 1°C. Overall, 1.5°C warming is associated with a 17% increase in the risk of precipitation extremes, and an additional 0.5°C warming further increases the risk of extreme precipitation by 19%.

Figure 3 displays maps of the risk ratios for 50-year events in a format similar to Figure 2. These maps look very similar to those of 20-year events shown in Figure 2. However, the magnitudes of the risk ratios for 50-year events at the same warming level are different; they are larger than the corresponding values for 20-year events if the event becomes more frequent in the warmer world but smaller than the corresponding values for 20-year events if the extremes become less frequent in the warmer world. The difference in the risk ratio between 50-year and 20-year events is larger at the 2°C warming level than at the 1.5°C warming level. Clearly, the relative changes in probability are larger for rarer, more extreme events. The difference in the risk ratios between 20-year and 10-year events (Figure S4) shows similar results, indicating once again that the relative changes in probability are larger for rarer, more extreme events.

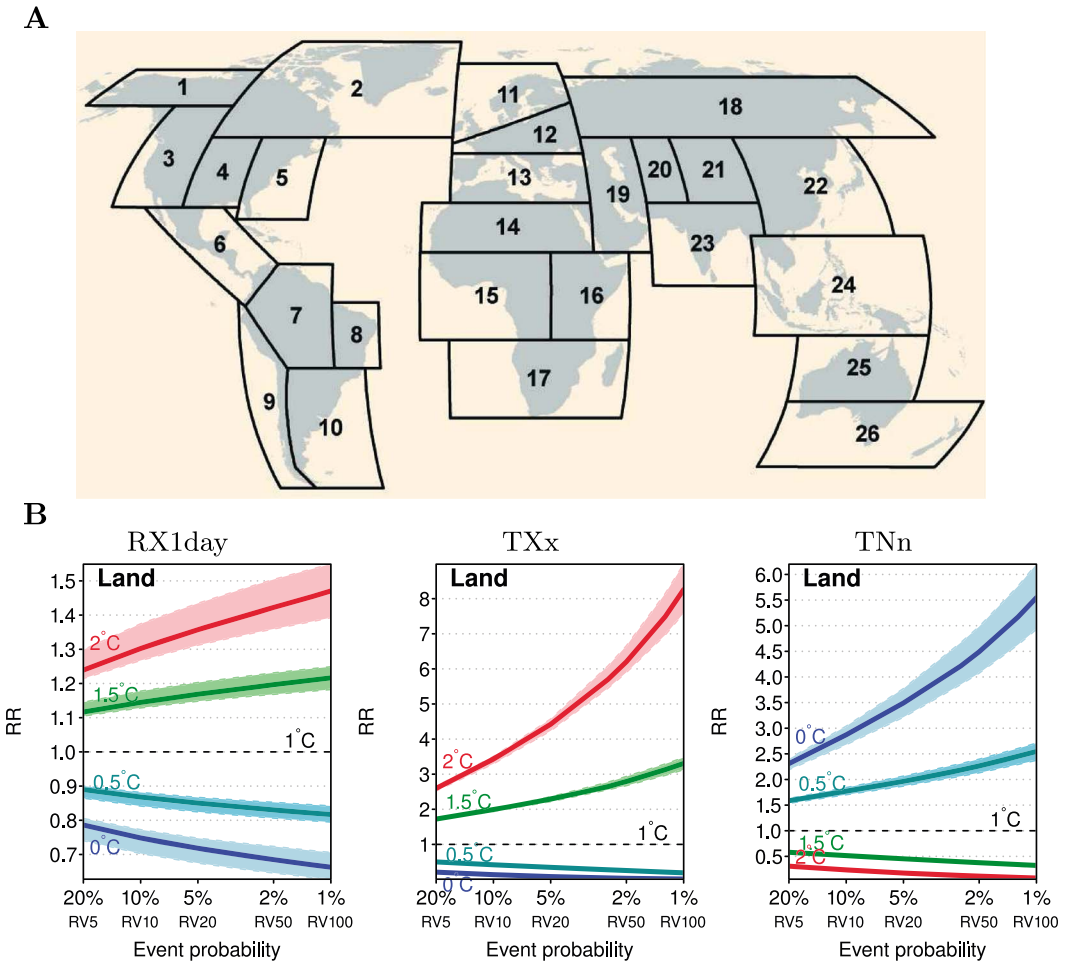

Figure 4. (a) Map showing the "SREX" regions (Figures 1–3 in Seneviratne et al., 2012) for which statistics are computed. (b) Risk ratios for precipitation extremes RX1day, warm extremes TXx, and cold extremes TNn over land for different event probabilities under 0.0°C (preindustrial), 0.5°C, 1.5°C, and 2°C global warming relative to event probabilities in the current climate (1°C global warming). The shading shows the multimodel interquartile (25%–75%) range.

Regional risk ratios can be very different from the median risk ratio over global land areas. Table 1 summarizes risk ratios for the 20- and 50-year events for regions used in the IPCC Special Report on Extremes (Seneviratne et al., 2012; Figure 4a) at different warming levels. To illustrate the regional results that are detailed in Table 1, we describe findings for two climatologically warm regions, East Africa and East Asia. These regions experience changes in risk ratios that are typical for land areas when comparing 20- and 50-year events.

Considering first 20-year extreme events, the increase in global temperature from 1°C to 1.5°C results in ~280% and ~90% increases in the risk ratio (relative frequency) of present-day climate 20-year warm extremes in the East Africa (from 1 to 3.82) and East Asia (from 1 to 1.86) regions, respectively. The additional 0.5°C global temperature increase beyond 1.5°C to 2.0°C leads to further increases in the risk ratio in the two regions by ~540% (from 3.82 to 9.22) and ~130% (from 1.86 to 3.17), respectively. Correspondingly, the frequency of 20-year cold extremes in these two regions declines by ~70% and ~50% with the increase in global temperature from 1°C to 1.5°C and further declines by another ~25% with the additional 0.5°C global temperature increase from 1.5°C to 2.0°C. The frequency of 20-year precipitation extremes in these regions increases by about 20–25% with each 0.5°C increase in global temperature. As modeled warming in the warm extremes is somewhat faster than observed, future increases in the frequency of current climate warm extremes could be smaller than reported here. On the contrary, modeled warming in the cold extremes is somewhat slower than observed; hence, future decreases in the frequency of cold extremes could be greater than reported here.

Table 1
Risk Ratio in Extreme Event Defined as the Ratio of the Event Probability at the Global Temperature Level Indicated in Column Headings (0, 1, 1.5, and 2°C Warmer Than Preindustrial) to the Probability in the Current Climate (Assumed to be 1°C Warmer Than Preindustrial)

a. Warm temperature extremes

	Tmax20					Tmax50				
Region	0.0°C	0.5°C	1°C	1.5°C	2.0°C	0.0°C	0.5°C	1°C	1.5°C	2.0°C
Alaska/N. W. Canada (1)	0.29	0.56	1	1.67	2.62	0.21	0.49	1	1.84	3.18
E. Canada/Greenl./Icel. (2)	0.23	0.51	1	1.79	2.96	0.16	0.43	1	2.04	3.75
W. North America (3)	0.07	0.33	1	2.31	4.50	0.03	0.24	1	2.87	6.38
C. North America (4)	0.14	0.41	1	2.03	3.58	0.06	0.31	1	2.46	4.99
E. North America (5)	0.12	0.38	1	2.21	4.25	0.08	0.32	1	2.60	5.67
Central America/Mexico (6)	0.05	0.29	1	2.67	5.86	0.02	0.21	1	3.32	8.44
Amazon (7)	0.00	0.14	1	3.58	8.37	0.00	0.07	1	4.78	13.9
N. E. Brazil (8)	0.00	0.10	1	4.10	10.2	0.00	0.04	1	5.61	17.6
W. Coast South America (9)	0.04	0.26	1	2.88	6.53	0.02	0.20	1	3.51	9.43
S. E. South America (10)	0.12	0.39	1	2.14	3.88	0.07	0.32	1	2.52	5.32
N. Europe (11)	0.26	0.53	1	1.73	2.79	0.17	0.45	1	1.97	3.51
C. Europe (12)	0.10	0.38	1	2.15	3.90	0.04	0.26	1	2.58	5.44
S. Europe/Mediterranean (13)	0.04	0.27	1	2.73	5.78	0.01	0.17	1	3.40	8.51
Sahara (14)	0.00	0.07	1	4.32	10.3	0.00	0.02	1	6.26	18.9
W. Africa (15)	0.01	0.16	1	3.49	8.53	0.00	0.10	1	4.58	13.4
E. Africa (16)	0.00	0.12	1	3.82	9.22	0.00	0.06	1	5.24	15.6
S. Africa (17)	0.01	0.19	1	3.08	6.96	0.00	0.12	1	3.98	10.7
N. Asia (18)	0.23	0.51	1	1.76	2.87	0.14	0.42	1	2.03	3.69
W. Asia (19)	0.01	0.16	1	3.35	7.73	0.00	0.09	1	4.50	12.8
C. Asia (20)	0.09	0.36	1	2.26	4.39	0.04	0.27	1	2.72	6.05
Tibetan Plateau (21)	0.15	0.41	1	2.09	3.90	0.10	0.35	1	2.45	5.17
E. Asia (22)	0.20	0.48	1	1.86	3.17	0.13	0.40	1	2.16	4.13
S. Asia (23)	0.03	0.26	1	2.60	5.38	0.01	0.16	1	3.34	7.95
S. E. Asia (24)	0.02	0.21	1	3.23	7.35	0.00	0.14	1	4.15	11.7
N. Australia (25)	0.06	0.30	1	2.49	5.06	0.02	0.21	1	3.12	7.25
S. Australia/New Zealand (26)	0.17	0.45	1	1.93	3.34	0.09	0.36	1	2.29	4.54
Globe	0.03	0.24	1	2.82	6.07	0.01	0.16	1	3.58	9.17
Land	0.09	0.35	1	2.29	4.43	0.04	0.26	1	2.77	6.17
Ocean	0.02	0.21	1	3.06	6.84	0.00	0.13	1	3.98	10.7
Canada	0.19	0.47	1	1.89	3.21	0.12	0.39	1	2.18	4.22

b. Cold temperature extremes (RR Tmin20)

	Tmin20					Tmin50				
Region	0.0°C	0.5°C	1°C	1.5°C	2.0°C	0.0°C	0.5°C	1°C	1.5°C	2.0°C
Alaska/N. W. Canada (1)	4.55	2.31	1	0.35	0.09	6.31	2.79	1	0.27	0.04
E. Canada/Greenl./Icel. (2)	5.38	2.58	1	0.29	0.05	7.85	3.20	1	0.21	0.02
W. North America (3)	2.52	1.63	1	0.58	0.31	3.03	1.80	1	0.51	0.23
C. North America (4)	2.51	1.64	1	0.56	0.28	3.13	1.86	1	0.48	0.20
E. North America (5)	3.87	2.11	1	0.39	0.12	5.31	2.53	1	0.30	0.05
Central America/Mexico (6)	3.03	1.81	1	0.50	0.23	3.77	2.04	1	0.43	0.16
Amazon (7)	4.32	2.14	1	0.44	0.18	4.78	2.27	1	0.42	0.17
N. E. Brazil (8)	6.08	2.80	1	0.27	0.05	8.32	3.33	1	0.22	0.03
W. Coast South America (9)	3.39	1.92	1	0.47	0.19	4.25	2.15	1	0.41	0.15
S. E. South America (10)	2.39	1.59	1	0.60	0.33	2.88	1.75	1	0.53	0.26
N. Europe (11)	3.96	2.15	1	0.38	0.11	5.54	2.62	1	0.29	0.05
C. Europe (12)	2.80	1.75	1	0.51	0.23	3.53	1.99	1	0.43	0.15
S. Europe/Mediterranean (13)	2.77	1.72	1	0.54	0.26	3.33	1.92	1	0.47	0.19
Sahara (14)	4.30	2.22	1	0.39	0.13	5.70	2.57	1	0.32	0.08
W. Africa (15)	5.61	2.62	1	0.30	0.06	7.86	3.16	1	0.23	0.03
E. Africa (16)	5.68	2.62	1	0.31	0.07	7.88	3.10	1	0.24	0.04
S. Africa (17)	3.92	2.10	1	0.41	0.14	5.10	2.42	1	0.35	0.09
N. Asia (18)	3.77	2.06	1	0.42	0.14	4.99	2.41	1	0.34	0.09
W. Asia (19)	2.74	1.70	1	0.55	0.29	3.25	1.87	1	0.49	0.22
C. Asia (20)	2.48	1.62	1	0.59	0.33	2.96	1.77	1	0.52	0.25
Tibetan Plateau (21)	2.38	1.58	1	0.61	0.35	2.81	1.72	1	0.55	0.28

Table 1 *(continued)*

b. Cold temperature extremes (RR Tmin20)

	Tmin20					Tmin50				
Region	0.0°C	0.5°C	1°C	1.5°C	2.0°C	0.0°C	0.5°C	1°C	1.5°C	2.0°C
E. Asia (22)	2.78	1.73	1	0.54	0.26	3.46	1.94	1	0.46	0.19
S. Asia (23)	3.46	1.94	1	0.46	0.19	4.40	2.22	1	0.39	0.13
S. E. Asia (24)	5.45	2.51	1	0.35	0.10	7.11	2.81	1	0.30	0.06
N. Australia (25)	4.08	2.15	1	0.39	0.11	5.54	2.57	1	0.29	0.06
S. Australia/New Zealand (26)	4.03	2.19	1	0.38	0.11	5.72	2.63	1	0.28	0.05
Globe	4.60	2.33	1	0.35	0.09	6.35	2.79	1	0.27	0.05
Land	3.47	1.96	1	0.46	0.18	4.45	2.25	1	0.38	0.12
Ocean	5.26	2.54	1	0.30	0.06	7.51	3.10	1	0.23	0.03
Canada	5.25	2.51	1	0.31	0.06	7.41	3.09	1	0.22	0.02

c. Precipitation extremes

	Pr20					Pr50				
Region	0.0°C	0.5°C	1°C	1.5°C	2.0°C	0.0°C	0.5°C	1°C	1.5°C	2.0°C
Alaska/N. W. Canada (1)	0.65	0.81	1	1.23	1.49	0.62	0.79	1	1.25	1.56
E. Canada/Greenl./Icel. (2)	0.61	0.79	1	1.26	1.55	0.57	0.76	1	1.30	1.66
W. North America (3)	0.73	0.86	1	1.16	1.34	0.69	0.83	1	1.19	1.41
C. North America (4)	0.69	0.84	1	1.19	1.39	0.65	0.81	1	1.23	1.49
E. North America (5)	0.62	0.79	1	1.24	1.52	0.58	0.77	1	1.29	1.64
Central America/Mexico (6)	0.77	0.88	1	1.13	1.28	0.73	0.86	1	1.16	1.34
Amazon (7)	0.68	0.83	1	1.20	1.42	0.62	0.79	1	1.24	1.53
N. E. Brazil (8)	0.66	0.82	1	1.21	1.44	0.61	0.78	1	1.26	1.56
W. Coast South America (9)	0.73	0.86	1	1.16	1.34	0.68	0.83	1	1.20	1.42
S. E. South America (10)	0.69	0.84	1	1.19	1.40	0.65	0.81	1	1.22	1.48
N. Europe (11)	0.67	0.82	1	1.21	1.45	0.64	0.80	1	1.23	1.51
C. Europe (12)	0.71	0.84	1	1.18	1.37	0.67	0.82	1	1.20	1.44
S. Europe/Mediterranean (13)	0.81	0.90	1	1.10	1.21	0.77	0.88	1	1.13	1.28
Sahara (14)	0.99	0.99	1	1.01	1.01	0.97	0.99	1	1.01	1.03
W. Africa (15)	0.71	0.85	1	1.17	1.37	0.69	0.83	1	1.20	1.43
E. Africa (16)	0.64	0.81	1	1.23	1.50	0.61	0.79	1	1.26	1.58
S. Africa (17)	0.75	0.87	1	1.15	1.30	0.71	0.85	1	1.17	1.37
N. Asia (18)	0.68	0.83	1	1.20	1.42	0.65	0.81	1	1.23	1.50
W. Asia (19)	0.81	0.90	1	1.10	1.22	0.78	0.89	1	1.12	1.26
C. Asia (20)	0.69	0.83	1	1.19	1.40	0.65	0.81	1	1.23	1.49
Tibetan Plateau (21)	0.68	0.83	1	1.20	1.42	0.65	0.81	1	1.23	1.50
E. Asia (22)	0.65	0.81	1	1.22	1.46	0.61	0.78	1	1.26	1.57
S. Asia (23)	0.63	0.80	1	1.23	1.50	0.60	0.78	1	1.27	1.60
S. E. Asia (24)	0.65	0.81	1	1.22	1.47	0.62	0.79	1	1.25	1.55
N. Australia (25)	0.85	0.92	1	1.08	1.17	0.83	0.91	1	1.09	1.20
S. Australia/New Zealand (26)	0.81	0.90	1	1.11	1.22	0.78	0.89	1	1.13	1.26
Globe	0.73	0.86	1	1.16	1.34	0.69	0.83	1	1.19	1.41
Land	0.72	0.85	1	1.17	1.36	0.68	0.83	1	1.20	1.43
Ocean	0.74	0.86	1	1.15	1.33	0.71	0.84	1	1.18	1.39
Canada	0.65	0.81	1	1.22	1.48	0.62	0.79	1	1.25	1.55

Note. In each section, results for 20-year and 50-year events from SREX regions are shown, along with the global and land values. The numbers in parentheses beside the region names correspond to the region numbering in Figure 4a.

Similar tendencies are seen when considering the rarer 50-year extreme events. For 50-year extreme warm events, the increase in risk ratios from 1.0°C to 1.5°C and from 1.5°C to 2.0°C global warming is nearly double the increase in risk ratio that was found for 20-year events. In contrast, for 50-year extreme cold events, decrease in risk ratio from 1.0°C to 1.5°C is slightly greater than that for less rare 20-year events, but further decline in risk ratio due to an additional 0.5°C warming is similar to that for 20-year events. The risk ratio for 50-year precipitation extremes increases by about a third in the same regions, which is again somewhat larger than that for 20-year events.

In general, the patterns of change in risk ratio with the rarity of event seen in these two regions mirror changes seen in other regions. The estimated magnitude of increase in the relative frequency (risk ratio) of hot events is very sensitive to the rarity of the event, with greater increases in relative frequency for rarer events. A similar, although much less pronounced, phenomenon is observed for extreme precipitation events. In contrast, the estimated magnitude of decrease in the relative frequency (risk ratio) of cold events is less sensitive to the rarity of the event. The probability of cold events that were formerly 20- or 50-year events at the 1.0°C level converges toward zero with further warming, and thus, the risk ratio also converges to zero and becomes insensitive to the further warming. This lack of sensitivity will, in fact, become apparent earlier for events that are rarer in the 1.0°C world. For cold events, the large reduction of event probabilities that already occur at the 1.5°C warming level leaves little room for additional reduction at the 2.0°C and higher levels of warming. Also, as is anticipated by the arguments above, risk ratios are smaller for 50-year cold events at both warming levels than the corresponding risk ratios for the 20-year cold events.

These features are displayed at a global scale in Figure 4b, which displays global land area median risk ratios for extreme precipitation and extreme temperatures of different return periods under different warming levels as compared to the current climate. Differences in the risk ratio values for different types of extremes and for different event probabilities are apparent. As the extreme value distributions shift to the right (Figure 1), risk ratios increase as event probability decreases, or in other words, relative changes in occurrence probability are larger for the more extreme events. This includes larger RR values for longer return periods (rarer events) in the case of increases in extremes such as RX1day and TXx and smaller RR values for longer return periods in the case of decreases in TNn, meaning that risk increases disproportionately for the additional 0.5°C for rarer events. Uncertainty increases correspondingly, as can be seen from the increase in the multimodel spread of RR values between the 1.5°C and 2.0°C global warming levels. It is also worth noting that the sensitivity of risk ratios for extreme warm and cold events to temperature change and rarity is reversed for global cooling relative to present-day climate. That is, risk ratios for extreme warm temperatures become insensitive to rarity for larger cooling levels, and those for extreme cold temperatures become increase rapidly with rarity (contrast the red and green curves in the middle and right-hand panels of Figure 4b that correspond to warming relative to the present with the cyan and blue curves that correspond to cooling).

4. Conclusions and Discussion

Historical extreme events, especially recent unprecedented events, are often used to assess human influence on extremes because of their association to high impacts (NAS, 2016). They have also been used to assess differential impacts at 1.5 and 2.0°C of global warming. For example, record high summer temperature and record low rainfall amount have been used to illustrate some of the differences in Australian climate extremes that could be expected in a 1.5°C or 2°C world (King et al., 2017). Here we showed that changes in the magnitude of risk ratio, which could be considered as a lower boundary for relative risk changes assuming that the consequences of extreme events will not decrease, are dependent on the rarity of the extreme event in the current climate as well as the amount of additional global warming beyond the present (with larger RR for rarer events). Substantially greater complexity for risk assessment will arise in the context of compound events (Leonard et al., 2014; Moftakhari et al., 2017; Wahl et al., 2015; Zheng et al., 2014). The implication is that risk assessment will depend critically on an understanding of the thresholds for the occurrence of extremes and kinds of extremes at which vulnerability increases sharply. Because different extremes will affect different sectors in very different ways, risk assessment will also depend critically on what society values and on the metrics of loss. In the absence of knowledge of the critical thresholds at which high vulnerability is produced (such that exposure would almost inevitably lead to loss), there is a significant danger of inadvertently overstating changes in risk by referencing levels thresholds for extremes above those critical levels, or conversely, of understating risk by referencing levels below those critical levels. One approach that might help to avoid overstating changes in risk may be to determine risk ratios not just for single events, but as a function of rarity, as in Figure 4. Such an approach would provide users with insights about how risk, as measured by simple risk ratios, varies with rarity and would assist users in weighing policy options by implicitly imposing the question, what level of rarity is critical for the system that is of concern.

While changes in risk ratio are dependent on the rarity of extreme event that is referenced, changes in the magnitude or return levels of extreme events may not be as sensitive, at least for extreme warm temperatures. This is a consequence of the nature of GEV distribution of the annual maximum temperature (TXx), for which change is dominated by change in the location parameter (e.g., Figure 1). This potentially brings about another dimension of complexity as to which metric, probability of fixed magnitude or magnitude at a fixed frequency, most effectively conveys information about changes in risk to users such as policy makers. Ultimately, the choice will be application dependent. For systems that fail when there is exceedance above a fixed threshold, the magnitude of exceedance may be secondary; in those cases, simple metrics that reflect changes in probability may be sufficient. On the other hand, for systems in which the extent of damage is dependent on both magnitude and frequency, for example, when larger changes in magnitude for a given event frequency lead to more extensive crop damage or larger numbers of people at risk, more complex metrics that recognize the impacts of change in both frequency and magnitude may be needed.

Acknowledgments
We appreciate Michael Wehner and an anonymous reviewer for their constructive comments. We acknowledge the World Climate Research Programme's Working Group on Coupled Modelling, which is responsible for CMIP, and we thank the climate modeling groups for producing and making available their model output. For CMIP, the U.S. Department of Energy's Program for Climate Model Diagnosis and Intercomparison provides coordinating support and led development of software infrastructure in partnership with the Global Organization for Earth System Science Portals. The CMIP5 data are available at http://cmip-pcmdi.llnl.gov/cmip5/availability.html. A FORTRAN used to fit a GEV distribution to GCM data is available from ftp://www.cccma.ec.gc.ca/pub/skharin/2018EF000813R/code/.

References

Coles, S. (2001). *An introduction to statistical modeling of extreme values*. London: Springer.

Donat, M. G., Alexander, L. V., Yang, H., Durre, I., Vose, R., Dunn, R. J. H., et al. (2013). Updated analyses of temperature and precipitation extreme indices since the beginning of the twentieth century: The HadEX2 dataset. *Journal of Geophysical Research: Atmospheres*, *118*, 2098–2118. https://doi.org/10.1002/jgrd.50150

Dunne, J. P., Stouffer, R. J., & John, J. G. (2013). Reductions in labour capacity from heat stress under climate warming. *Nature Climate Change*, *3*, 563–566. https://doi.org/10.1038/nclimate1827

Easterling, D. R., Meehl, G. A., Parmesan, C., Changnon, S. A., Karl, T. R., & Mearns, L. O. (2000). Climate extremes: Observations, modeling, and impacts. *Science*, *289*, 2068–2074. https://doi.org/10.1126/science.289.5487.2068

Handmer, J., Honda, Y., Kundzewicz, Z. W., & Mechler, R. (2012). Changes in impacts of climate extremes: Human systems and ecosystems. In C. B. Field, et al. (Eds.), *Managing the risks of extreme events and disasters to advance climate change adaptation A Special Report of Working Groups I and II of the Intergovernmental Panel on Climate Change (IPCC)* (pp. 231–290). Cambridge, UK, and New York, NY, USA: Cambridge University Press.

IPCC (2012). In C. B. Field, et al. (Eds.), *Managing the risks of extreme events and disasters to advance climate change adaptation. A special report of working groups I and II of the Intergovernmental Panel on Climate Change* (p. 582). Cambridge, UK, and New York, NY, USA: Cambridge University Press.

Kharin, V. V., Zwiers, F. W., Zhang, X., & Wehner, M. (2013). Changes in temperature and precipitation extremes in the CMIP5 ensemble. *Climatic Change*, *119*, 345–357. https://doi.org/10.1007/s10584-013-0705-8

Kim, Y.-H., Min, S.-K., Zhang, X., Zwiers, F., Alexander, L. V., Donat, M. G., & Tung, Y.-S. (2016). Attribution of extreme temperature changes during 1951–2010. *Climate Dynamics*, *46*, 1769–1782. https://doi.org/10.1007/s00382-015-2674-2

King, A. D., Karoly, D. J., & Henley, B. J. (2017). Australian climate extremes at 1.5°C and 2°C of global warming. *Nature Climate Change*, *7*, 412–416. https://doi.org/10.1038/nclimate3296

Leonard, M., Westra, S., Phatak, A., Lambert, M., van den Hurk, B., McInnes, K., et al. (2014). A compound event framework for understanding climate extreme impacts. *WIREs Climate Change*, *5*(1), 113–128. https://doi.org/10.1002/wcc.252

Lesk, C., Coffel, E., D'Amato, A. W., Dodds, K., & Horton, R. (2017). Threats to North American forests from southern pine beetle with warming winters. *Nature Climate Change*. https://doi.org/10.1038/NCLIMATE3375

Li, C., Zhang, X., Zwiers, F., Fang, Y., & Michalak, A. (2017). Recent very hot summers in northern hemispheric land areas measured by wet bulb globe temperature will be the norm within 20 years. *Earth's Future*. https://doi.org/10.1002/2017EF000639

Min, S.-K., Zhang, X., Zwiers, F. W., & Hegerl, G. C. (2011). Human contribution to more intense precipitation extremes. *Nature*, *470*, 378–381. https://doi.org/10.1038/nature09763

Moftakhari, H. R., Salvadori, G., AghaKouchak, A., Sanders, B. F., & Matthew, R. A. (2017). Compounding effects of sea level rise and fluvial flooding. *Proceedings of the National Academy of Sciences*, *114*, 9785–9790. https://doi.org/10.1073/pnas.1620325114

National Academies of Sciences, Engineering, and Medicine (2016). *Attribution of extreme weather events in the context of climate change*. Washington, DC: The National Academies Press. https://doi.org/10.17226/21852

Oppenheimer, M., Campos, M., Warren, R., Birkmann, J., Luber, G., O'Neill, B., & Takahashi, K. (2014). Emergent risks and key vulnerabilities. In C. B. Field, et al. (Eds.), *Climate change 2014: Impacts, adaptation, and vulnerability. Part A: Global and sectoral aspects. Contribution of working group II to the fifth assessment report of the Intergovernmental Panel on Climate Change* (pp. 1039–1099). Cambridge, United Kingdom and New York, NY, USA: Cambridge University Press.

Pal, J. S., & Eltahir, E. A. B. (2015). Future temperature in southwest Asia projected to exceed a threshold for human adaptability. *Nature Climate Change*, *6*, 197–200. https://doi.org/10.1038/nclimate2833

Rogelj, J., Luderer, G., Pietzcker, R. C., Kriegler, E., Schaeffer, M., Krey, V., & Riahi, K. (2015). Energy system transformations for limiting end-of-century warming to below 1.5°C. *Nature Climate Change*, *5*, 519–527. https://doi.org/10.1038/nclimate2572

Seneviratne, S. I., Donat, M. G., Pitman, A. J., Knutti, R., & Wilby, R. L. (2016). Allowable CO_2 emissions based on regional and impact-related climate targets. *Nature*, *529*, 477–483. https://doi.org/10.1038/nature16542

Seneviratne, S. I., Nicholls, N., Easterling, D., Goodess, C. M., Kanae, S., & Kossin, J. (2012). Changes in climate extremes and their impacts on the natural physical environment. In C. B. Field, et al. (Eds.), *Managing the risks of extreme events and disasters to advance climate change adaptation A Special Report of Working Groups I and II of the Intergovernmental Panel on Climate Change (IPCC)* (pp. 109–230). Cambridge, UK, and New York, NY, USA: Cambridge University Press.

Sillmann, J., Kharin, V. V., Zhang, X., Zwiers, F. W., & Bronaugh, D. (2013). Climate extremes indices in the CMIP5 multimodel ensemble, part 1: Model evaluation in the present climate. *Journal of Geophysical Research: Atmospheres*, *118*, 1716–1733. https://doi.org/10.1002/jgrd.50203

Taylor, K. E., Stouffer, R. J., & Meehl, G. A. (2012). An overview of CMIP5 and the experiment design. *Bulletin of the American Meteorological Society*, *93*, 485–498. https://doi.org/10.1175/BAMS-D-11-00094.1

United Nations Framework Convention on Climate Change (2015). Twenty-first session of the conference of parties, Paris. Article 2 of the Paris Agreement (FCCC/CP/2015/10/Add.1) downloaded 25 February 2016 from http://unfccc.int/resource/docs/2015/cop21/eng/10a01.pdf

van Vuuren, D. P., Edmonds, J., Kainuma, M., Riahi, K., Thomson, A., Hibbard, K., et al. (2011). The representative concentration pathways: An overview. *Climatic Change*, *109*(1-2), 5–31. https://doi.org/10.1007/s10584-011-0148-z

Wahl, T., Jain, S., Bender, J., Meyers, S. D., & Luther, M. E. (2015). Increasing risk of compound flooding from storm surge and rainfall for major U.S. cities. *Nature Climate Change*, *5*, 1093–1097. https://doi.org/10.1038/nclimate2736

Westra, S., Alexander, L., & Zwiers, F. (2013). Global Increasing trends in annual maximum daily precipitation. *Journal of Climate*, *26*, 3904–3917. https://doi.org/10.1175/JCLI-D-12-00502.1

World Meteorological Organization (2017). WMO statement on the state of the global climate in 2016. WMO-No. 1189, 1–28.

Zhang, X., Wan, H., Zwiers, F. W., Hegerl, G. C., & Min, S.-K. (2013). Attributing intensification of precipitation extremes to human influence. *Geophysical Research Letters*, *40*, 5252–5257. https://doi.org/10.1002/grl.51010

Zheng, F., Westra, S., Leonard, M., & Sisson, S. A. (2014). Modeling dependence between extreme rainfall and storm surge to estimate coastal flooding risk. *Water Resources Research*, *50*, 2050–2071. https://doi.org/10.1002/2013WR014616

Zwiers, F. W., Zhang, X., & Feng, Y. (2011). Anthropogenic influence on long return period daily temperature extremes at regional scales. *Journal of Climate*, *24*, 881–892. https://doi.org/10.1175/2010JCLI3908.1